hexagon:2611.00815v1

PROOFS OF TWO CONJECTURES OF FOMIN AND PYLYAVSKYY

Abstract. We prove Conjecture 8.12 of Fomin and Pylyavskyy on direction independence of their cluster structures. We also prove their surface Conjecture 5: the natural map from the tensor-diagram skein algebra to the ring of SL_3-invariants is an isomorphism.

1. Introduction

Let V be a three-dimensional complex vector space with a nonzero alternating form $\mathrm{vol} : V^3 \to \mathbb{C}$, and let $\mathrm{SL}(V)$ be the group preserving this form. Fix a basis e_1, e_2, e_3 with $\mathrm{vol}(e_1, e_2, e_3) = 1$ and its dual basis e_1^*, e_2^*, e_3^*. For $a, b, c \in \mathbb{N} = \{0, 1, \ldots\}$, the invariant rings

$$R_{a,b,c}(V) = \mathbb{C}[(V^*)^a \times V^b \times \mathrm{SL}(V)^c]^{\mathrm{SL}(V)} \tag{1.1}$$

combine invariants of vectors and covectors with invariants of matrices. An element $g \in \mathrm{SL}(V)$ sends a vector v to gv, a covector α to αg^{-1}, and a matrix X to gXg^{-1}. For an affine variety X, we write $\mathcal{O}(X) = \mathbb{C}[X]$ for its coordinate ring.

For $c = 0$, the first fundamental theorem of invariant theory expresses these invariants through pairings and the volume forms on V and V^*; see Weyl [16]. Tensor diagrams record their contractions: edges pair a vector and a covector, and trivalent vertices carry a volume tensor. We denote the resulting invariant of a diagram D by $[D]$. Kuperberg's A_2 spider [10] gives local relations among these diagrams and planar web bases for the corresponding invariant tensor spaces. Thus algebraic identities can be studied by resolving crossings and reducing small faces. When $a = c = 0$ and $b \geq 3$, the determinants are the Plücker coordinates, and $R_{0,b,0}(V)$ is the homogeneous coordinate ring of $\mathrm{Gr}(3, b)$.

Fomin and Zelevinsky introduced cluster algebras in connection with total positivity and dual canonical bases [5]. Starting from an algebraically independent set of functions, their exchange relations produce further such sets, called clusters. Scott [12] constructed cluster structures on Grassmannian coordinate rings. Fomin and Pylyavskyy extended this construction to the mixed vector–covector rings in their 2012 preprint, published as [3]. A cyclic black-and-white signature σ records the order of the arguments: black entries label vectors and white entries label covectors. Their special invariants associate functions to boundary points and triangles, and triangulations produce mutation-equivalent seeds. The resulting polynomial cluster algebra is the whole invariant ring [3, Theorem 8.1].

A cyclic signature is non-alternating if two cyclically adjacent entries have the same color. For these signatures, the definition of the special invariants uses a direction around the boundary in constructing caterpillar diagrams and their proxy vertices. Fomin and Pylyavskyy proved that interchanging the colors preserves the cluster structure [3, Theorem 8.11] and asked, in Conjecture 8.12, whether reversing the chosen direction does so as well.

Write $R_\sigma(V) = R_{a,b,0}(V)$ when σ has a white and b black entries, with its arguments labelled by σ, and let $\mathcal{C}_\sigma^+$ denote the structure constructed in [3]. Let $\mathcal{C}_\sigma^-$ denote the mirror construction: the caterpillars, proxy vertices, and connections used to define the special invariants are reflected,

Date: November 21, 2026.

2020 *Mathematics Subject Classification.* Primary 13F60; Secondary 13A50, 57K31.

Key words and phrases. Cluster algebra, tensor diagram, invariant ring, skein algebra.

while tensor diagrams are evaluated with the same fixed volume form and vertex convention. The two structures are compared as structures on the same labelled ring.

Theorem 1.1 (Direction independence)**.** *Let σ be a non-alternating cyclic signature of length at least five. Then*

$$\mathcal{C}_\sigma^+ = \mathcal{C}_\sigma^-.$$

More precisely, the two constructions have the same frozen variables, the same cluster variables, the same clusters, and the same exchange relations. Their quivers agree up to simultaneous reversal of the arrows incident to each connected component of the mutable part, as allowed in the original construction.

Theorem 1.1 proves that conjecture in its stated range. Fomin and Pylyavskyy's cross-product embeddings realize these rings as cluster subalgebras of an all-black Grassmannian ring [3, Theorem 8.9]. Reflection is a cluster symmetry of the Grassmannian; see Fraser [6, Section 5]. We compare the two colored structures inside this common ambient structure.

Cao and Li's denominator criterion detects compatibility of cluster variables, and their connectivity theorem controls mutations retaining a fixed collection of variables [1]. Their unistructurality theorem identifies clusters from the set of cluster variables [2]. Here the comparison begins with equality of embedded polynomial subrings. We prove that freezing and deletion recover the smaller extended-variable set by intersecting the ambient set with that subring, and that compatibility is inherited as well. The support-reduction form of this descent argument appears in [14, Lemma 2.1 and Theorem 2.2]; Section 2 gives the general statement and reconstructs the exchange data. A calculation with volume signs then makes reflection commute with the cross-product embedding, proving Theorem 1.1.

The surface question has a parallel invariant-theoretic origin. Sikora [13] described rings of SL_n-representation invariants by graphs and local relations, including the matrix-invariant case. Fomin and Pylyavskyy [4] placed trivalent tensor diagrams on bordered surfaces and included vector and covector arguments at boundary points. Let S be a compact connected oriented surface of genus g with $h \geq 1$ boundary components. Let $M \subset \partial S$ be a finite labelled set, and let $\sigma : M \to \{\circ, \bullet\}$ color a points white and b points black. Each boundary component has its induced cyclic order. Cutting S to a disk requires

$$c = 2g + h - 1 \tag{1.2}$$

cuts. A diagram is evaluated by assigning a covector to each white point, a vector to each black point, and an element of $\mathrm{SL}(V)$ to each cut. Denote the tensor-diagram skein algebra by $\mathcal{W}_\sigma(S)$. It is the quotient by the relations of Figures 4–5 in [4]; these relations are recalled in Section 4. Theorem 4 of that paper gives a surjective homomorphism

$$\phi : \mathcal{W}_\sigma(S) \longrightarrow R_{a,b,c}(V). \tag{1.3}$$

Their Conjecture 5 asks whether this map is injective.

Theorem 1.2 (Surface evaluation)**.** *For every surface and every boundary signature described above, the homomorphism* (1.3) *is an isomorphism.*

The theorem includes arbitrary colors, unmarked boundary components, and $M = \varnothing$.

Frohman and Sikora [7] introduced the reduced $SU(3)$-skein algebra with ordered boundary endpoints and established a basis of reduced webs. Their Section 13 relates the Fomin–Pylyavskyy map to decorated local systems and formulates a stronger conjecture. The reduced algebra admits two endpoint degrees at each boundary interval, recording the two edge directions. Keeping only one direction at each colored point is the fixed-color construction considered by Ishibashi and Yuasa [9, Remark 2.18]; in the classical disk case it recovers $R_\sigma(V)$.

Ishibashi and Yuasa [9, Theorem 2] embedded the boundary-localized $\mathfrak{sl}_3$ skein algebra into the corresponding quantum cluster algebra. Ishibashi, Oya, and Shen [8, Theorems 2 and 4.3] identified its classical specialization with the cluster algebra and the regular functions on the generic decorated-local-system space. These results apply to triangulable unpunctured marked surfaces with a mark on each boundary component and at least two marks in total. A decorated SL_3 flag carries both a nonzero vector v and a nonzero covector α satisfying $\alpha(v) = 0$; the boundary localization imposes genericity between neighboring decorations. The original map (1.3) instead uses the prescribed vector or covector at each colored point and its polynomial invariant ring. Comparing these presentations requires the boundary relations and the evaluation maps.

For stated skeins, Lê and Sikora [11] proved a bigon decomposition and an embedding of the reduced $SU(3)$-skein algebra obtained by assigning an extreme state to every endpoint. Wang [15, Theorems 1.1 and 1.4] constructed the classical evaluation on groupoid representations and identified its kernel with the nilradical. His Corollary 5.16 gives an isomorphism when the fundamental group is free and the marking is nonempty, as in the surface case used here.

We deduce Theorem 1.2 from the skein theorems of Lê and Sikora, giving the comparisons for the original fixed-color quotient and the original map ϕ. The full nonnegative endpoint grading identifies that quotient with a subalgebra of the reduced skein algebra. A system of saturated arcs gives a direct proof of the surface case of Wang's faithful evaluation, with explicit matrix coordinates. Finally, a single boundary rescaling matches the trivalent tensor conventions. Auxiliary intervals on unmarked boundary components are handled by their degree-zero part.

Sections 2–3 prove Theorem 1.1; Sections 4–6 prove Theorem 1.2. All tensor products and coordinate rings are over $\mathbb{C}$. Numbered statements cited from papers with a specified preprint version refer to that version.

2. Polynomial cluster subalgebras

2.1. **Conventions.** A seed of geometric type consists of an algebraically independent extended cluster $z = (x_1, \dots, x_n, f_1, \dots, f_s)$ and an integer matrix $\widetilde{B} = (b_{ij})$ of size $(n+s) \times n$. The first n variables form the mutable cluster, and the f_j are frozen; adjoining all frozen variables gives the extended cluster. The principal part $(b_{ij})_{1 \le i,j \le n}$ is skew-symmetrizable: positive integers d_i satisfy $d_i b_{ij} = -d_j b_{ji}$. Mutation in a mutable direction k replaces x_k by

$$x_k' = \frac{\prod_{b_{ik}>0} z_i^{b_{ik}} + \prod_{b_{ik}<0} z_i^{-b_{ik}}}{x_k}, \tag{2.1}$$

and changes the matrix by

$$b_{ij}' = \begin{cases} -b_{ij}, & i = k \text{ or } j = k, \\ b_{ij} + [b_{ik}]_+[b_{kj}]_+ - [-b_{ik}]_+[-b_{kj}]_+, & \text{otherwise,} \end{cases} \qquad [u]_+ = \max(u, 0). \tag{2.2}$$

The polynomial cluster algebra is the $\mathbb{C}$-subalgebra of $\mathbb{C}(z)$ generated by all mutable variables obtained by mutation and by the frozen variables, as in [3, 4].

For a cluster structure $\mathcal{C}$, write $\mathrm{EV}(\mathcal{C})$ for the union of its mutable and frozen variables in the ambient field. We also write $\mathrm{EV}(A)$ when the structure on an algebra A is specified. Two such variables are compatible if they lie in a common extended cluster; compatibility with oneself is understood.

Definition 2.1. Starting from a seed, freeze a subset of its mutable variables. Then delete any chosen vertices having no edge to a mutable vertex, together with their variables; equivalently, their matrix entries in every remaining mutable column are zero. The polynomial cluster algebra of the resulting seed is called a cluster subalgebra. This is Definition 8.7 of [3].

A mutable vertex that will be deleted can first be frozen. Freezing removes its mutable column from the exchange matrix; deletion then removes its variable and its matrix row.

2.2. **Compatibility theorems.** Fix a mutable cluster $x = (x_1, \dots, x_n)$. For a cluster variable u, let $d_j(u)$ be minus the least exponent of x_j in its reduced Laurent expansion relative to x. The Laurent coefficients may lie in the field of the original frozen variables. We use the following results of Cao and Li:

(i) $d_j(u) = -1$ precisely when $u = x_j$; $d_j(u) = 0$ precisely when $u \neq x_j$ and u, x_j are compatible; otherwise $d_j(u) > 0$ [1, Theorem 6.3].
(ii) Every finite collection of pairwise compatible mutable variables belongs to a cluster [1, Theorem 7.4].
(iii) Seeds whose clusters contain a specified collection of variables form a connected subgraph of the exchange graph [1, Theorem 6.2].
(iv) Two distinct clusters with $n - 1$ common mutable variables differ by one mutation [1, Corollary 7.6].

These statements apply to the seed patterns above through the following coefficient description. For any seed, including a seed obtained by freezing, let $\mathbb{P} = \mathrm{Trop}(f_1, \dots, f_s)$ be the multiplicative group of Laurent monomials in its frozen variables, with

$$\Big(\prod_j f_j^{u_j}\Big) \oplus \Big(\prod_j f_j^{v_j}\Big) = \prod_j f_j^{\min(u_j, v_j)} \qquad (u_j, v_j \in \mathbb{Z}).$$

Set $y_k = \prod_j f_j^{b_{n+j,k}}$. Then

$$\frac{y_k}{1 \oplus y_k} = \prod_j f_j^{[b_{n+j,k}]_+}, \qquad \frac{1}{1 \oplus y_k} = \prod_j f_j^{[-b_{n+j,k}]_+}. \tag{2.3}$$

The normalized exchange relation is

$$x_k x_k' = \frac{y_k \prod_{i=1}^n x_i^{[b_{ik}]_+} + \prod_{i=1}^n x_i^{[-b_{ik}]_+}}{1 \oplus y_k}.$$

Substituting (2.3) gives (2.1). Its coefficient mutation is

$$y_k' = y_k^{-1}, \qquad y_i' = y_i\, y_k^{[b_{ki}]_+} (1 \oplus y_k)^{-b_{ki}} \quad (i \neq k).$$

This agrees with (2.2): for integers u, v,

$$u[v]_+ - \min(u, 0)v = [u]_+[v]_+ - [-u]_+[-v]_+,$$

as follows by writing $u = [u]_+ - [-u]_+$ and $v = [v]_+ - [-v]_+$. The left side is the change in a frozen exponent under normalized coefficient mutation; the right side is its change in the extended matrix. Thus the same variables and clusters occur in both descriptions. The polynomial algebra remains the $\mathbb{C}$-algebra generated by the extended variables.

Proposition 2.2 (Descent)**.** *Let $B \subset A$ be a cluster subalgebra in the sense of Definition 2.1, with the indicated polynomial structures. Then*

$$\mathrm{EV}(B) = \mathrm{EV}(A) \cap B. \tag{2.4}$$

For every finite subset $T \subset \mathrm{EV}(B)$, the following are equivalent:

(a) T is contained in an extended cluster of B;
(b) T is contained in an extended cluster of A.

Proof. Choose an ambient seed defining the inclusion. Partition its mutable index set as $I \sqcup J$, where I consists of the directions remaining mutable in B. Put every original mutable variable eventually deleted into J. Let E be the full set of deleted vertices, and let K be the set of retained extended vertices. The smaller seed has extended cluster $(z_k)_{k\in K}$ and matrix $(b_{ki})_{k\in K, i\in I}$. The deletion condition says

$$b_{ei} = 0 \qquad (e \in E,\ i \in I). \tag{2.5}$$

This zero block is preserved by mutation at any $k \in I$: if $i = k$, formula (2.2) negates zero; otherwise every correction to b_{ei} contains $b_{ek} = 0$. Induction proves preservation along every sequence in I. Thus these ambient mutations use only retained variables and are the mutations of the smaller seed. In particular,

$$B \subset \mathbb{C}(z_k : k \in K). \tag{2.6}$$

Each mutable generator of B is obtained along a sequence in I. It is therefore compatible in A with every initial variable x_j, $j \in J$. Each retained variable newly made frozen has the same property. An original ambient frozen variable has exponent zero in all mutable directions. By (i), every generator of B has a Laurent expansion with no negative exponent in any x_j, $j \in J$. The Laurent polynomials with this property form a subring. Hence every element of B has this property.

Suppose an ambient mutable variable u lies in B. Then $d_j(u) \le 0$ for every $j \in J$, so u is compatible with each x_j. By (ii), there is an ambient cluster containing u and all these x_j. By (iii), it is reachable from the chosen initial seed through seeds retaining all of J. Along such a path no variable of J is mutated: a mutation replaces its variable by a different variable and would remove it from the cluster. Algebraic independence prevents the removed variable from remaining under another label. Thus the path uses only I.

If u is not one of the x_j, this path produces it as a mutable variable of B. If $u = x_j$, it must be retained, and is then frozen in B. Indeed, a deleted initial variable cannot belong to the field in (2.6), by algebraic independence of the initial extended cluster. The same field argument handles an original ambient frozen variable lying in B: it must be retained. This proves the inclusion $\mathrm{EV}(A) \cap B \subset \mathrm{EV}(B)$. The reverse inclusion follows from the realization by mutations in I.

The implication (a)⇒(b) follows from that realization as well. For the converse, remove the original ambient frozen variables from T and call the remaining set T_0. Its elements are ambient mutable variables. They are pairwise compatible by (b), and each is compatible with every x_j, $j \in J$, because each belongs to $\mathrm{EV}(B)$. Therefore $T_0 \cup \{x_j : j \in J\}$ is pairwise compatible. By (ii) and (iii), a cluster containing this union can be reached by mutations in I. Deleting E from the resulting seed gives an extended cluster of B containing T. Original ambient frozen variables in T were retained throughout. □

Lemma 2.3. *The composition of two cluster-subalgebra inclusions is a cluster-subalgebra inclusion.*

Proof. Suppose $B \subset A$ and $D \subset B$ are obtained by freezing and deletion. The seed of B at which the second operation is performed is reached by mutations in the directions retained at the first step. Lift these mutations to A. The first deleted block remains zero by (2.2). Freeze the additional directions and delete the additional vertices used to obtain D. A vertex deleted at the second step has no adjacency to the finally mutable directions, and every vertex deleted at the first step still has no such adjacency. Both operations are therefore a single freezing and deletion at the lifted ambient seed. □

Corollary 2.4 (Uniqueness inside an ambient structure)**.** *Suppose two polynomial cluster structures on a subring $B \subset A$ are both obtained from the same skew-symmetric ambient structure by freezing and deletion. Then they have the same extended variables, frozen variables, clusters, and exchange relations. Their exchange matrices differ at most by reversal on connected components of the mutable part.*

Proof. Proposition 2.2 determines the extended-variable set as $\mathrm{EV}(A) \cap B$, and determines its compatibility relation from A.

A frozen variable is compatible with every extended variable. Conversely, if $x = x_k$ is mutable, its exchange partner x' has a nonzero numerator independent of x_k in (2.1). Hence $d_k(x') = 1$, so x and x' are incompatible. Thus the frozen variables are exactly the elements compatible with all extended variables. This determines the mutable set as well.

For either structure, a pairwise compatible mutable set has size at most its mutable rank: a larger finite subset would contradict (ii). The frozen set is finite. Every pairwise compatible extended set is therefore finite, and (ii) identifies its maximal members with the extended clusters. The two structures have identical extended clusters.

Fix such a cluster and a mutable variable x. Its exchange partner in the first structure produces a cluster that also occurs in the second. By (iv), it is the exchange partner of x in the second structure. The product xx' is the same function in the two structures. Algebraic independence of the remaining extended variables makes its polynomial expansion unique, so the unordered pair of exchange monomials is identical. The two monomials have disjoint supports; if they coincide, both are one. Reading their exponent vectors therefore determines each exchange column up to its sign.

Write the two extended matrices in this cluster as (b_{ij}) and $(\widehat{b}_{ij})$. For each column choose $\epsilon_j \in \{1, -1\}$ with $\widehat{b}_{ij} = \epsilon_j b_{ij}$. For mutable i, j, skew-symmetry gives

$$\epsilon_j b_{ij} = \widehat{b}_{ij} = -\widehat{b}_{ji} = -\epsilon_i b_{ji} = \epsilon_i b_{ij}.$$

Thus $\epsilon_i = \epsilon_j$ whenever $b_{ij} \neq 0$, and the signs are constant on the connected components of the mutable part. A zero column gives $xx' = 2$ and is determined as well. At mutable rank zero, the extended-variable set is the unique extended cluster. □

3. Reflection and cross products

3.1. **Cross-product embeddings.** For a labelled signature σ, let X_σ be the product of copies of V at black positions and copies of V^* at white positions. Then $R_\sigma(V) = \mathbb{C}[X_\sigma]^{\mathrm{SL}(V)}$. For $u, v, w \in V$, set

$$(u \times v)(w) = \mathrm{vol}(u, v, w).$$

Replace every white position by two consecutive black positions. The resulting all-black signature β has length $N = 2a + b$. Write (u_p, v_p) for the pair replacing a white position p, in clockwise boundary order. Define

$$F_\sigma : X_\beta \longrightarrow X_\sigma \tag{3.1}$$

by retaining the original black vectors and replacing each pair (u_p, v_p) by $u_p \times v_p$. For $g \in \mathrm{SL}(V)$,

$$((gu) \times (gv))(w) = \mathrm{vol}(gu, gv, w) = \mathrm{vol}(u, v, g^{-1}w) = (u \times v)(g^{-1}w),$$

so F_σ is equivariant. To express a nonzero covector α as a cross product, choose w with $\alpha(w) = 1$ and a basis u, v of $\ker \alpha$. Rescale u so that $\mathrm{vol}(u, v, w) = 1$. The covectors $u \times v$ and α agree on the basis u, v, w, hence are equal. The zero covector is $0 \times v$. Making these choices independently at each white position proves that F_σ is surjective. Its pullback is therefore injective:

$$\Phi_\sigma = F_\sigma^* : R_\sigma(V) \hookrightarrow R_\beta(V). \tag{3.2}$$

We use the following results of [3]. Theorem 8.1 identifies the polynomial cluster algebra of the special-invariant seeds with $R_\sigma(V)$, independently of the triangulation. Theorem 8.9 says that a cross-product map for two consecutive equal colors gives a cluster subalgebra in the sense of Definition 2.1. Theorem 8.5 identifies the all-black structure with Scott's structure on the homogeneous coordinate ring of $\mathrm{Gr}(3, N)$. At each expansion of a white point, the new signature has consecutive black entries, so it is non-alternating. The initial signature is non-alternating by hypothesis. Repeated use of Theorem 8.9 and Lemma 2.3 therefore gives

$$\Phi_\sigma(\mathcal{C}_\sigma^+) \subset \mathcal{G}_\beta, \tag{3.3}$$

where $\mathcal{G}_\beta$ denotes the all-black Grassmannian cluster structure.

3.2. **Signs under reflection.** Let σ^{r} and β^{r} be the reversed labelled signatures of σ and β, respectively. Define

$$\tau_\sigma : X_\sigma \longrightarrow X_{\sigma^{\mathrm{r}}}, \qquad (z_1, \ldots, z_{a+b}) \longmapsto (-z_{a+b}, \ldots, -z_1), \tag{3.4}$$

where each z_i is a vector or a covector according to its color. Its pullback is

$$M_\sigma = \tau_\sigma^* : R_{\sigma^{\mathrm{r}}}(V) \longrightarrow R_\sigma(V).$$

Lemma 3.1. *Let D be a tensor diagram with signature σ^{r}, and let rD be its reflection with signature σ. With the tensor conventions of* [3]*,*

$$[rD] = M_\sigma([D]). \tag{3.5}$$

Consequently,

$$\mathcal{C}_\sigma^- = M_\sigma(\mathcal{C}_{\sigma^{\mathrm{r}}}^+). \tag{3.6}$$

Proof. At a trivalent vertex the tensor is the alternating volume tensor, or its dual, with ports read clockwise. Reflection reverses the cyclic order and contributes a factor -1 at each internal vertex. Vertex-free circles are unchanged by reflection and may be omitted from the half-edge count. For the remaining graph, let t be the number of internal vertices, d the total boundary degree, and e the number of edges. Counting half-edges gives

$$3t + d = 2e,$$

so $t \equiv d \pmod 2$. Reversing the arguments accounts for the reflected boundary labels. Negating every argument contributes $(-1)^d = (-1)^t$. This proves (3.5). Isolated boundary points have degree zero, and the argument applies componentwise if the diagram is disconnected.

Reflection carries the clockwise caterpillars and their proxy vertices to the counterclockwise ones, and carries their central connections and triangulations to the reflected connections and triangulations. Hence it transports the special invariants used in each seed. Propositions 6.4–6.6 of [3] factor the nonzero special invariants into irreducible special invariants by identities with coefficient one. Reflecting these identities and applying (3.5) gives the same factorization procedure for the reflected diagrams, including the coefficient-one normalization of the factors in Definition 7.1 of that paper.

Finally, applying the ring isomorphism M_σ to each exchange identity preserves both monomials and their coefficients. It therefore carries the original seeds and all their mutations to the mirror seeds. This proves (3.6). □

Lemma 3.2. *The configuration maps satisfy*

$$F_{\sigma^{\mathrm{r}}} \circ \tau_\beta = \tau_\sigma \circ F_\sigma. \tag{3.7}$$

Equivalently, their pullbacks satisfy

$$\Phi_\sigma \circ M_\sigma = M_\beta \circ \Phi_{\sigma^{\mathrm{r}}}. \tag{3.8}$$

Proof. At an original black position both compositions give the negative of the vector. At a white position the pair (u, v) becomes $(-v, -u)$ after reflection, and

$$(-v) \times (-u) = v \times u = -(u \times v).$$

The identities at all positions prove (3.7). Pulling back reverses the arrows and gives (3.8). □

Proof of Theorem 1.1. For $\mathrm{Gr}(3, N)$ the signed reversal (3.4) is the usual twisted reflection. It sends frozen variables to frozen variables and clusters to clusters, and reverses the exchange quiver; see [6, Section 5]. Thus

$$M_\beta(\mathcal{G}_{\beta^{\mathrm{r}}}) = \mathcal{G}_\beta.$$

By (3.3), $\Phi_\sigma(\mathcal{C}_\sigma^+)$ is a cluster subalgebra of $\mathcal{G}_\beta$. By Lemmas 3.1 and 3.2,

$$\Phi_\sigma(\mathcal{C}_\sigma^-) = M_\beta(\Phi_{\sigma^{\mathrm{r}}}(\mathcal{C}_{\sigma^{\mathrm{r}}}^+))$$

is another cluster subalgebra of $\mathcal{G}_\beta$: a cluster automorphism transports freezing and deletion. Both structures have exactly the same underlying subring

$$\Phi_\sigma(R_\sigma(V)) \subset R_\beta(V).$$

Corollary 2.4 identifies them. Injectivity of Φ_σ gives equality of the two structures on $R_\sigma(V)$.

The component reversals are those in Definition 7.10 of [3]. The proof includes the exceptional five-point signatures of mutable rank one with six frozen variables. □

4. Boundary colors and skein relations

4.1. **Tensor diagrams on a bordered surface.** Let S and σ be as in Theorem 1.2. A tensor diagram is a finite graph drawn on S, with crossings permitted, whose internal vertices are trivalent sources or sinks. Sources are white and sinks are black. Every boundary vertex is one of the prescribed marked points; its incident edges point into the surface at a white point and out of the surface at a black point. Several edges may end at one marked point. Oriented closed curves without vertices are also allowed. The cyclic order at an internal vertex is supplied by the orientation of S.

Choose oriented cuts $\gamma_1, \ldots, \gamma_c$ from unmarked boundary points to unmarked boundary points, so that cutting along them gives a disk. On the disk, assign an alternating volume tensor to each trivalent vertex and contract along edges. At a black marked point insert the corresponding vector once for each incident edge; at a white marked point insert the corresponding covector. An edge crossing γ_j inserts X_j or X_j^{-1}, according to the crossing direction. A vertex-free closed curve is evaluated by the trace of its holonomy. In the fixed volume-normalized basis, the vertex coefficients are

$$\varepsilon_{ijk} = \begin{cases} \mathrm{sgn}(i, j, k), & \{i, j, k\} = \{1, 2, 3\}, \\ 0, & \text{otherwise}, \end{cases}$$

read in the clockwise cyclic order. These rules define a polynomial invariant $[D] \in R_{a,b,c}(V)$. The entries of X_j^{-1} are polynomial on $\mathrm{SL}(V)$, since $\det X_j = 1$.

4.2. **The original skein quotient.** The vector space $\mathcal{W}_\sigma(S)$ is generated by tensor diagrams modulo isotopy and the local relations of [4, Figures 4–5]. We recall them to fix the quotient and the signs. A contractible circle equals 3; an internal digon equals -2 times the straight edge; an internal square is the sum of its two resolutions. A crossing is the sum of the uncrossed diagram and the two-vertex diagram. A digon attached to one boundary vertex is zero, with either choice of color. These relations are shown in Figure 1. The usual Reidemeister moves are allowed, and interchanging two ports at a trivalent vertex changes its sign. All rotations and orientation reversals of a displayed relation are included.

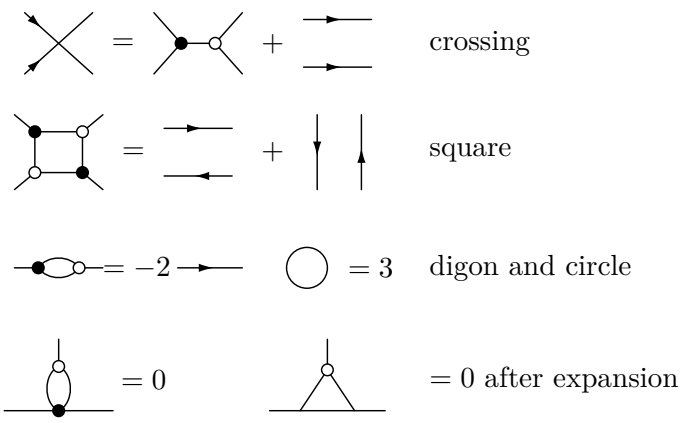


FIGURE 1. The local relations at the classical parameter. Edges point from white vertices to black vertices; arrows on univalent portions complete the orientation. In the last row the horizontal line is the surface boundary. The left diagram has one clasped marked point, and the right diagram has two endpoints on its expanded interval. Color-reversed relations are included.

All indices in the following tensor calculations lie in $\{1,2,3\}$, and δ_{ij} is the Kronecker delta. The alternating tensor satisfies

$$\sum_r \varepsilon_{ijr}\varepsilon_{klr} = \delta_{ik}\delta_{jl} - \delta_{il}\delta_{jk}. \tag{4.1}$$

If either index pair repeats, both sides are zero. Otherwise a nonzero summand requires the two pairs to have the same complementary index; the sign is positive for equal ordered pairs and negative for reversed pairs. This proves (4.1).

With the external ports ordered as in the crossing relation, the two-vertex tensor H has entries

$$H_{ij}^{kl} = \sum_r \varepsilon_{ijr}\varepsilon_{rlk} = \delta_{il}\delta_{jk} - \delta_{ik}\delta_{jl}. \tag{4.2}$$

Thus $H = P - I$, where $P(v \otimes w) = w \otimes v$ and I is the identity. Since $P^2 = I$,

$$H^2 = 2I - 2P = -2H, \qquad H(v \otimes v) = 0, \qquad P = I + H. \tag{4.3}$$

The circle and digon contractions are

$$\sum_i \delta_{ii} = 3, \qquad \sum_{u,v} \varepsilon_{iuv}\varepsilon_{jvu} = -2\delta_{ij}.$$

For the square, label the external ports i,j,k,l clockwise from the upper left and the internal edges x,y,z,w in the same order. Its contraction is

$$\sum_{x,y,z,w} \varepsilon_{ixw}\varepsilon_{jyx}\varepsilon_{kzy}\varepsilon_{lwz}.$$

First sum over x in (4.1), obtaining $\delta_{iy}\delta_{wj} - \delta_{ij}\delta_{wy}$. The remaining contraction is

$$\begin{aligned}\sum_z \varepsilon_{kzi}\varepsilon_{ljz} - \delta_{ij}\sum_{y,z}\varepsilon_{kzy}\varepsilon_{lyz} &= (-\delta_{ij}\delta_{kl} + \delta_{il}\delta_{jk}) + 2\delta_{ij}\delta_{kl} \\ &= \delta_{ij}\delta_{kl} + \delta_{il}\delta_{jk},\end{aligned}$$

the two square resolutions. For $v = \sum_j v_j e_j$, a boundary fork vanishes because $\sum_{j,k}\varepsilon_{ijk}v_jv_k = 0$; interchanging j,k negates the coefficient and preserves v_jv_k. The dual calculation is identical.

Antisymmetry of ε gives the port-interchange relation. The flip satisfies $P^2 = I$ and the braid relation, and a curl resolves as $3 - 2 = 1$. These give the Reidemeister relations in [4, Figure 5].

Multiplication in $\mathcal{W}_\sigma(S)$ is superposition of diagrams. The relations make it a commutative algebra, and evaluation gives the homomorphism ϕ of (1.3).

4.3. **Expanding the marked points.** On each boundary component with no marked point, insert one auxiliary point, called a dummy point. Choose one boundary ideal point between every pair of consecutive marked or dummy points, and remove the ideal points from S to obtain Σ. If a boundary component has just one marked or dummy point, choose one other point on that component as its ideal point. Write $E_0, \dots, E_{m-1}$ for the connected components of $\partial\Sigma$. Each is an open interval containing exactly one original or dummy point, and $m \geq 1$. Expanding a marked point means separating its incident endpoints along its interval. The surface Σ has only boundary ideal points.

Let $RS(\Sigma)$ denote the reduced skein algebra of Frohman and Sikora [7, Sections 3–4], specialized at $q = a_{\mathrm{FS}} = 1$, where a_{FS} denotes their boundary parameter. It is generated by oriented ribbon webs with distinct ordered endpoints on the intervals. At E_i, let $d_i^{\mathrm{in}}(D)$ and $d_i^{\mathrm{out}}(D)$ count the endpoints pointing into and out of the surface. The defining interior relations specialize to those above. In addition, the boundary cap and the boundary fork are zero. Their boundary H relation straightens the length-three path joining two adjacent opposite-direction endpoints; its coefficient is $a_{\mathrm{FS}}^{\pm 1} = 1$. In the notation of [7], these are relations (4) and (5).

All these relations are homogeneous in the full endpoint degree

$$\deg D = \left(d_i^{\mathrm{in}}(D), d_i^{\mathrm{out}}(D)\right)_{i=0}^{m-1} \in \mathbb{N}^{2m}.$$

For a black interval retain only outward-pointing endpoints, and for a white interval retain only inward-pointing endpoints. At a dummy interval retain degree zero in both directions. These conditions define a coordinate face $P_\sigma \subset \mathbb{N}^{2m}$. Set

$$B_\sigma = \bigoplus_{\gamma \in P_\sigma} RS(\Sigma)_\gamma. \tag{4.4}$$

Here $RS(\Sigma)_\gamma$ is the homogeneous component of degree γ. The space B_σ is a subalgebra, since P_σ is closed under addition.

Lemma 4.1 (Comparison of boundary conventions)**.** *Expanding marked points induces an isomorphism*

$$\kappa : \mathcal{W}_\sigma(S) \xrightarrow{\sim} B_\sigma. \tag{4.5}$$

Proof. The free vector space of web diagrams is graded by $\mathbb{N}^{2m}$. Its relation subspace is spanned by homogeneous local relations inserted into diagrams on the fixed surface. Such insertion preserves the actual endpoints of a boundary relation on $\partial\Sigma$; the context adds nonnegative endpoint degrees. A positive forbidden coordinate therefore remains positive in every context. Projecting onto the degrees in P_σ retains exactly the contextual relations of degrees in that face. Thus restriction to the face commutes with taking the quotient.

The surviving relations, including their orientation reversals, compare as follows. The interior loop, digon, square, and crossing relations coincide, with digon coefficient -2. A boundary cap has opposite-direction endpoints, so it is absent on the face. The same is true of the boundary H relation. A boundary fork has two endpoints with the same direction. After these are clasped at their original point, it is the boundary digon set to zero in [4, Figure 4(e)]. The two pictures in which all three edges end at the same boundary point follow by applying the fork relation to two adjacent endpoints, with the third edge in the surrounding context. Degree zero at a dummy interval permits only diagrams and relations with no endpoint there.

At $q = 1$ the two choices of crossing have the same skein expansion, so projection to S and lifts to the thickening give the same quotient. To check the vertex and twist conventions within this quotient, resolve the crossing that interchanges two adjacent ports at a trivalent vertex: the terms are the original vertex and its digon multiple, giving $1 - 2 = -1$. A curl resolves into a circle term and a digon term, giving $3 - 2 = 1$. Together with the crossing relation, these give the local vertex and Reidemeister relations above.

It remains to check the linear order of endpoints. Interchanging two adjacent endpoints of the same direction gives a crossing. Resolving it produces the original order and a term with a boundary fork. The latter is zero. Every permutation is a product of adjacent transpositions, so all choices of order have the same class. We may therefore expand a clasped boundary vertex to distinct ordered endpoints in any order, and we may clasp them again without a choice.

These operations preserve all surviving relations in both directions. Their composites are the identity on diagrams modulo the relations and the endpoint permutations just verified. They give inverse homomorphisms between $\mathcal{W}_\sigma(S)$ and B_σ. □

5. Classical evaluation of stated skeins

5.1. **The published skein inputs.** Let $\mathcal{S}_3(\Sigma; 1)$ be the stated SL_3-skein algebra of Lê and Sikora at $v = 1$, so that their parameter $q = v^6$ is also one. A state assigns a label in $\{1, 2, 3\}$ to each boundary endpoint. The diagrams are oriented ribbon graphs in the thickening of Σ, modulo the interior and boundary relations of [11, Section 4]. We use the following statements over the ground ring $\mathbb{C}$:

(i) Giving every endpoint state 3 defines a linear injection

$$\eta : RS(\Sigma) \hookrightarrow \mathcal{S}_3(\Sigma; 1). \tag{5.1}$$

Its image is a direct summand. This is [11, Theorem 11.6], with $a_{\mathrm{FS}} = 1$.

(ii) For an oriented bigon $\mathbb{B}$ there is a Hopf algebra isomorphism

$$\Psi : \mathcal{O}(\mathrm{SL}_3) \xrightarrow{\sim} \mathcal{S}_3(\mathbb{B}; 1) \tag{5.2}$$

that sends a matrix entry to the corresponding stated arc [11, Theorem 6.3].

(iii) Let $\mathcal{A} = \{a_1, \ldots, a_r\}$ be a saturated collection of pairwise disjoint compact oriented arcs properly embedded in Σ. Here saturated means that every complementary component contains exactly one ideal point and that the collection is maximal with this property. Write $U(a_j)$ for a small open bigon neighborhood of a_j. Along each boundary interval of Σ, order the incident bigon sides opposite to the boundary orientation. Place these sides in successive height blocks, preserving the internal endpoint order on each side. This is the negative boundary ordering of [11, Sections 5.4 and 8.4]. The inclusion of these neighborhoods induces a linear isomorphism

$$F_{\mathcal{A}} : \mathcal{O}(\mathrm{SL}_3)^{\otimes r} \xrightarrow{\Psi^{\otimes r}} \mathcal{S}_3\Big(\coprod_j U(a_j); 1\Big) \xrightarrow{\sim} \mathcal{S}_3(\Sigma; 1), \tag{5.3}$$

where

$$r = c + m - 1. \tag{5.4}$$

This is [11, Theorem 8.8].

These results hold over $\mathbb{C}$ at $v = 1$. We use the linear injection in (i) and the linear isomorphism in (iii).

5.2. **The groupoid represented by the arcs.** We choose a saturated system explicitly. Take c disjoint proper cuts with endpoints in the intervals, away from the ideal points, which cut S to a disk. The resulting disk has m boundary ideal points. Around $m-1$ of them choose disjoint small half-disks whose closures avoid the cut sides and their endpoints. Add the interior semicircular side of each half-disk to the cuts. These arcs have endpoints on the original boundary intervals and descend to disjoint proper arcs in Σ. Their complement consists of m disks, each with one boundary ideal point. Any additional disjoint proper arc lies in one such disk and separates it into two pieces, one with no ideal point. The system is therefore saturated. It has $c+m-1$ arcs, proving (5.4). Orient these arcs and call the resulting system $\mathcal{A}$.

Choose $p_i \in E_i$ for $0 \le i < m$, and let

$$\Pi = \pi_1(\Sigma; \{p_0, \dots, p_{m-1}\})$$

be the fundamental groupoid on these objects. Its morphisms are homotopy classes of paths with the specified endpoints. A representation H assigns matrices acting on column vectors, with

$$H(\beta \circ \gamma) = H(\beta)H(\gamma), \qquad H(\gamma^{-1}) = H(\gamma)^{-1},$$

where $\beta \circ \gamma$ means first γ, then β. Write $\mathrm{Rep}(\Pi, \mathrm{SL}_3)$ for the space of these representations. Frames at the objects are part of the data.

Lemma 5.1. *The arcs of $\mathcal{A}$, joined to the p_i within their boundary intervals, freely generate Π. Consequently,*

$$\mathrm{Rep}(\Pi, \mathrm{SL}_3) \cong \mathrm{SL}_3^r, \tag{5.5}$$

with independent matrix coordinates given by their holonomies.

Proof. Truncate a sufficiently small half-disk neighborhood of each ideal point, avoiding the compact arcs. The resulting compact core K has the same homotopy type as Σ. By the construction of $\mathcal{A}$, its complementary pieces are disks with one truncated boundary ideal point each.

After cutting K along the arcs, each piece is a closed disk Q with one distinguished new boundary segment c_Q from the truncation. The disk has a strong deformation retraction onto

$$\partial Q \setminus \mathrm{int}(c_Q)$$

fixing this remaining boundary. For instance, identify Q with a polygonal disk and successively collapse from the distinguished side. The remaining boundary is a closed interval, so these collapses fix every side belonging to a saturated arc or an original boundary interval. The retractions on the pieces therefore glue along their common arc sides.

It follows that K retracts onto the union of the saturated arcs and the surviving original boundary intervals. Each original interval is a tree containing its marked basepoint and the endpoints of all incident arcs. Contract these disjoint trees. The resulting graph has m vertices and r edges, one edge for each a_j. Contraction preserves the fundamental groupoid on the chosen objects. The groupoid of a graph is freely generated by its oriented edges: every path reduces by cancellation of an edge followed by its inverse, and there are no further relations. Thus the matrix on every a_j may be prescribed independently. This proves (5.5). □

5.3. **The tensor evaluation.** Extend the frame at p_i along the contractible interval E_i by parallel transport. For a diagram edge directed from its left endpoint to its right endpoint, transport the vector at the right endpoint back to the left, where it pairs with the covector; the dual operation handles the reversed direction. At internal vertices contract using the classical

stated tensors. At boundary endpoints use the vectors or covectors specified by their states. This defines the tensor evaluation

$$E : \mathcal{S}_3(\Sigma; 1) \longrightarrow \mathcal{O}(\mathrm{Rep}(\Pi, \mathrm{SL}_3)). \tag{5.6}$$

In the conventions of [11, Sections 2–3], the positive basis is e_1, e_2, e_3, and the negative basis at $v = 1$ is

$$f_i = (-1)^{i-1} e^*_{4-i} = e_i^* C, \qquad C = \begin{pmatrix} 0 & 0 & 1 \\ 0 & -1 & 0 \\ 1 & 0 & 0 \end{pmatrix}. \tag{5.7}$$

Here $C^2 = I$ and $\det C = 1$. Evaluation and coevaluation are the usual duality maps, crossing is the flip, and the pivotal sign is $(-1)^{3-1} = 1$. The trivalent tensors are the nonzero alternating tensors of the stated convention.

We verify the boundary relations [11, (47)–(50)]. The cap and completeness identities are

$$f_i(e_j) = (-1)^{i-1} \delta_{4-i,j}, \tag{5.8}$$

$$\sum_{i=1}^{3} (-1)^{i-1} e_i \otimes f_{4-i} = \sum_{i=1}^{3} e_i \otimes e_i^* = I_V. \tag{5.9}$$

The second equality uses $(-1)^{i-1}(-1)^{3-i} = 1$; interchanging the factors gives its dual. In the height-exchange relation (50), the term containing $q - q^{-1}$ vanishes and the remaining coefficient is one. It is therefore the flip.

In (47), the scalar denoted by a in [11] equals one and the permutation coefficient $(-q)^{\ell(\pi)}$ is $\mathrm{sgn}(\pi)$, where S_3 is the permutation group of $\{1, 2, 3\}$ and $\ell(\pi)$ is the number of inversions of π. The displayed top-to-bottom port order is $\pi(3), \pi(2), \pi(1)$. Its alternating tensor is consequently

$$\sum_{\pi \in S_3} \mathrm{sgn}(\pi) e_{\pi(3)} \otimes e_{\pi(2)} \otimes e_{\pi(1)} = - \sum_{\pi \in S_3} \mathrm{sgn}(\pi) e_{\pi(1)} \otimes e_{\pi(2)} \otimes e_{\pi(3)}.$$

This is the determinant expansion in that port order. The opposite orientation has the dual expansion in the f_i; it has the same determinant normalization because $\det C = 1$. These are the two orientations of (47). The interior relations are the flip and alternating-tensor identities, with the contractions in (4.1)–(4.3) and the square calculation above; see also [11, Section 3.4].

Trivialize the local system on a small disk supporting a relation. The preceding identities show that its evaluation is zero. A change of trivialization inserts mutually inverse basis changes on contracted edges. Thus (5.6) is well defined. Superposition produces disjoint tensor contractions, so $E(D_1 D_2) = E(D_1)E(D_2)$ and $E(1) = 1$; hence E is an algebra homomorphism. Its values are regular: the contractions are polynomials in matrix entries and inverse matrix entries, and the latter are cofactors on SL_3.

The following statement is the surface case of [15, Corollary 5.16]. We give a proof using (5.3) and the coordinates of Lemma 5.1.

Lemma 5.2 (Faithfulness of classical evaluation)**.** *The map E in* (5.6) *is injective.*

Proof. For the jth oriented bigon, choose the matrix coordinate Y_j so that transport from its right endpoint frame to its left endpoint frame is CY_j. Since $C \in \mathrm{SL}_3$ and $C^2 = I$, this is an invertible algebraic coordinate choice. Lemma 5.1 makes the Y_j independent.

In the following formulas, E is applied after the prescribed boundary-ordered inclusion of this bigon into Σ. Evaluation preserves products under this inclusion, since boundary height exchanges are flips. Let u^i_k be the matrix-entry function on SL_3. The generator $\Psi(u^i_k)$ in [11, Figure 12(c)] is directed from left to right, with state i on the left and state k on the right. Its evaluation is

$$E\Psi(u^i_k) = f_i(CY_j e_k) = e_i^* C^2 Y_j e_k = (Y_j)_{ik}. \tag{5.10}$$

The functions u_k^i generate $\mathcal{O}(\mathrm{SL}_3)$, so this identifies evaluation on the whole bigon algebra.

For $F_j \in \mathcal{O}(\mathrm{SL}_3)$, evaluation on the disjoint bigon neighborhoods gives

$$EF_{\mathcal{A}}(F_1 \otimes \cdots \otimes F_r) = \prod_{j=1}^{r} F_j(Y_j). \tag{5.11}$$

The prescribed boundary ordering gives the same product, since height exchange is the flip at $q = 1$. The right-hand side of (5.11) is the coordinate-ring isomorphism $\mathcal{O}(\mathrm{SL}_3)^{\otimes r} \cong \mathcal{O}(\mathrm{SL}_3^r)$. Pure tensors span the tensor product, so $EF_{\mathcal{A}}$ is a linear isomorphism. As $F_{\mathcal{A}}$ is a linear isomorphism, E is injective.

If $r = 0$, both spaces in (5.3) are $\mathbb{C}$ and the same proof is the identity on constants. This includes the one-interval disk. □

6. Proof of the surface conjecture

6.1. **Matching the vertex conventions.** We compare the original and stated volume tensors.

Lemma 6.1. *Keep the identity edge and the evaluation pairing fixed. Suppose the original and stated conventions assign nonzero alternating tensors to trivalent sources and sinks and satisfy the same digon relation with coefficient -2. Then there is a fixed $\nu \in \mathbb{C}^\times$ such that stated evaluation equals original evaluation after replacing each black boundary vector by ν times that vector and each white boundary covector by ν^{-1} times that covector.*

Proof. The spaces $\bigwedge^3 V$ and $\bigwedge^3 V^*$ are one-dimensional. Thus the stated source tensor is λ times the original source tensor, and the stated sink tensor is μ times the original sink tensor, for $\lambda, \mu \in \mathbb{C}^\times$. A digon contains one source and one sink; its other side is -2 times the fixed identity edge. Comparing the two digon identities gives $\lambda\mu = 1$.

For a diagram, let s and t count its internal sources and sinks, and let $d_\bullet, d_\circ$ be the total degrees at black and white boundary vertices. Counting outgoing minus incoming half-edges gives

$$3(s - t) = d_\bullet - d_\circ. \tag{6.1}$$

Write $\mathrm{ev}_{\mathrm{st}}$ and $\mathrm{ev}_{\mathrm{orig}}$ for the two tensor evaluations with the same boundary arguments. Multilinearity of contraction gives

$$\mathrm{ev}_{\mathrm{st}}(D) = \lambda^s \mu^t \, \mathrm{ev}_{\mathrm{orig}}(D) = \lambda^{s-t} \, \mathrm{ev}_{\mathrm{orig}}(D).$$

Choose ν with $\nu^3 = \lambda$. By (6.1), the multiplier is $\nu^{d_\bullet - d_\circ}$, the effect of the asserted boundary rescaling. This rescaling is fixed for all diagrams, multiplicative, and equivariant for $\mathrm{SL}(V)$. A component with no boundary has $s = t$ and multiplier one. □

Both calculi have the classical duality pairing, and their interior relations agree by [11, Theorem 11.6]. We use the fixed ν from Lemma 6.1 below.

6.2. **Frames and the original parameter space.** Use p_0 as basepoint and choose the cuts from the original evaluation disjoint from the p_i. In the cut disk choose paths $\rho_i : p_i \to p_0$, with ρ_0 constant. For each paired cut side, take a based loop crossing that side once and otherwise lying in the disk. Orient each loop so that its vector transport is the matrix inserted at the original X_j-labelled cut crossing. These loops form a free basis $\ell_1, \ldots, \ell_c$ of $\pi_1(S, p_0)$. A representation H determines

$$X_j = H(\ell_j), \qquad g_i = H(\rho_i), \qquad g_0 = I.$$

Conversely, for a path $\gamma : p_i \to p_j$, let w_γ be the reduced word representing the based loop $\rho_j \circ \gamma \circ \rho_i^{-1}$ in the ℓ_k. Then

$$H(\gamma) = g_j^{-1} w_\gamma(X_1^{\pm 1}, \dots, X_c^{\pm 1}) g_i. \tag{6.2}$$

For composable paths, the middle $g_j g_j^{-1}$ cancels and their based words multiply in the same order. Reversal gives the inverse matrix. Thus (6.2) defines the inverse parametrization. Both parametrizations are regular, since they use finite products and inverses of SL_3 matrices. In the disk trivialization determined by the ρ_i, transport away from cuts is the identity and gluing across the jth cut inserts X_j or X_j^{-1}.

Under the all-state-3 map (5.1), an interval with outgoing boundary direction supplies e_3, whereas the opposite direction supplies $f_3 = e_1^*$, by (5.7). Thus in the base frame the original arguments are

$$v_i = \nu g_i e_3 \quad \text{at a black interval,} \qquad \alpha_i = \nu^{-1} e_1^* g_i^{-1} \quad \text{at a white interval.} \tag{6.3}$$

Each original interval supplies its prescribed argument, and dummy intervals supply none.

Substitution of (6.3) and the cut holonomies defines an algebra homomorphism

$$\delta : R_{a,b,c}(V) \longrightarrow \mathcal{O}\big(\mathrm{Rep}(\Pi, \mathrm{SL}_3)\big). \tag{6.4}$$

It is regular because inverse matrices are regular on SL_3. The choice of a base frame only fixes a simultaneous SL_3 gauge; the functions on the left are invariant under that simultaneous action.

Proposition 6.2. *The comparison maps satisfy the identity*

$$E\eta\kappa = \delta\phi. \tag{6.5}$$

Proof. It suffices to check a tensor diagram D, since their classes span $\mathcal{W}_\sigma(S)$. Compute $\mathrm{ev}_{\mathrm{orig}}(D)$ using the original tensors, the vectors $g_i e_3$ at black intervals, and the covectors $e_1^* g_i^{-1}$ at white intervals. Across cuts use the matrices X_j and their inverses. These are the same edge transports as in E; uncut portions insert the identity, and vertex-free closed curves give holonomy traces.

Expansion and η give the stated contraction with these unscaled boundary arguments, because all endpoints have state 3. Lemma 6.1 therefore gives the first equality below. Rescaling the arguments as in (6.3) gives the second by multilinearity:

$$E\eta\kappa(D) = \nu^{d_\bullet - d_\circ}\, \mathrm{ev}_{\mathrm{orig}}(D) = \delta\phi(D).$$

The equality holds as a regular function for each diagram and therefore for every linear combination. □

Proof of Theorem 1.2. Lemma 4.1 makes κ an isomorphism. The map η is injective by [11, Theorem 11.6], and E is injective by Lemma 5.2. Therefore the left-hand side of (6.5) is injective. If $\phi(w) = 0$, then

$$E\eta\kappa(w) = \delta\phi(w) = 0,$$

and the three injections give $w = 0$. Thus ϕ is injective.

Surjectivity is [4, Theorem 4]. Explicitly, the invariant generators in its Theorem 1 are of the forms

$$\mathrm{tr}(W), \qquad \alpha_i(W v_j), \qquad \mathrm{vol}(W_1 v_i, W_2 v_j, W_3 v_k), \qquad \mathrm{vol}^*(\alpha_i W_1, \alpha_j W_2, \alpha_k W_3),$$

where the W, W_1, W_2, W_3 are matrix words in the X_j, and vol^* is the dual volume form on V^*. They are represented by closed curves, two-ended paths, and source or sink tripods. Paths can cross the cuts in any prescribed word, and intersections of paths are allowed. Thus every invariant generator is the image of a diagram.

The dummy intervals and the degree-zero restriction in Lemma 4.1 handle every unmarked boundary component. When $M = \varnothing$, all intervals are dummy and the factor $\nu^{d_\bullet - d_\circ}$ is one. The one-interval disk has $r = 0$, and the bigon has $r = 1$, so both are included in (5.3). Thus ϕ is an isomorphism for every surface and signature in Theorem 1.2. □

References

[1] P. Cao and F. Li, *The enough g-pairs property and denominator vectors of cluster algebras*, Math. Ann. **377** (2020), 1547–1572. doi:10.1007/s00208-020-02033-1. Numbering: arXiv:1803.05281v2.

[2] P. Cao and F. Li, *Unistructurality of cluster algebras*, Compos. Math. **156** (2020), 946–958. doi:10.1112/S0010437X20007113. arXiv:1809.05116v2.

[3] S. Fomin and P. Pylyavskyy, *Tensor diagrams and cluster algebras*, Adv. Math. **300** (2016), 717–787. doi:10.1016/j.aim.2016.03.030. Numbering: arXiv:1210.1888v4.

[4] S. Fomin and P. Pylyavskyy, *Webs on surfaces, rings of invariants, and clusters*, Proc. Natl. Acad. Sci. USA **111** (2014), no. 27, 9680–9687. doi:10.1073/pnas.1313068111. arXiv:1308.1718v1.

[5] S. Fomin and A. Zelevinsky, *Cluster algebras I: Foundations*, J. Amer. Math. Soc. **15** (2002), 497–529. arXiv:math/0104151.

[6] C. Fraser, *Braid group symmetries of Grassmannian cluster algebras*, Selecta Math. (N.S.) **26** (2020), Paper No. 17, 51 pp. doi:10.1007/s00029-020-0542-3. Numbering: arXiv:1702.00385v3.

[7] C. Frohman and A. S. Sikora, *SU(3)-skein algebras and webs on surfaces*, Math. Z. **300** (2022), 33–56. Numbering: arXiv:2002.08151v2.

[8] T. Ishibashi, H. Oya, and L. Shen, $\mathcal{A} = \mathcal{U}$ *for cluster algebras from moduli spaces of G-local systems*, Adv. Math. **431** (2023), 109256. doi:10.1016/j.aim.2023.109256. Numbering: arXiv:2202.03168v3.

[9] T. Ishibashi and W. Yuasa, *Skein and cluster algebras of unpunctured surfaces for* $\mathfrak{sl}_3$, Math. Z. **303** (2023), Paper No. 72. doi:10.1007/s00209-023-03208-7. Numbering: arXiv:2101.00643v4.

[10] G. Kuperberg, *Spiders for rank* 2 *Lie algebras*, Comm. Math. Phys. **180** (1996), 109–151. arXiv:q-alg/9712003.

[11] T. T. Q. Lê and A. S. Sikora, *Stated* $\mathrm{SL}(n)$*-skein modules and algebras*, J. Topol. **17** (2024), no. 3, e12350. doi:10.1112/topo.12350. Numbering: arXiv:2201.00045v3.

[12] J. S. Scott, *Grassmannians and cluster algebras*, Proc. London Math. Soc. (3) **92** (2006), 345–380. arXiv:math/0311148.

[13] A. S. Sikora, SL_n*-character varieties as spaces of graphs*, Trans. Amer. Math. Soc. **353** (2001), no. 7, 2773–2804. doi:10.1090/S0002-9947-01-02700-3. arXiv:math/9806016v2.

[14] Q. Tang, *Counting low-degree cluster variables in Grassmannians*, preprint (2026). aiXiv:2611.00582.

[15] Z. Wang, *The classical limit for stated* SL_n*-skein modules*, preprint (2024). Numbering: arXiv:2401.14753v1.

[16] H. Weyl, *The classical groups: their invariants and representations*, Princeton University Press, Princeton, NJ, 1939.